

Exclusive open-charm near-threshold cross sections in a coupled-channel approach

T. V. Uglov

Lebedev Physics Institute, 119991, Leninsky prospect 53, Moscow, Russia
National Research Nuclear University MEPhI, 115409, Kashirskoe highway 31, Moscow, Russia
Moscow Institute of Physics and Technology, 141700, Institutsky lane 9, Dolgoprudny, Moscow Region, Russia

Yu. S. Kalashnikova

Institute of Theoretical and Experimental Physics, 117218, B.Cheremushkinskaya 25, Moscow, Russia
National Research Nuclear University MEPhI, 115409, Kashirskoe highway 31, Moscow, Russia

A. V. Nefediev

Institute for Theoretical and Experimental Physics, 117218, B.Cheremushkinskaya 25, Moscow, Russia
National Research Nuclear University MEPhI, 115409, Kashirskoe highway 31, Moscow, Russia
Moscow Institute of Physics and Technology, 141700, Institutsky lane 9, Dolgoprudny, Moscow Region, Russia

G. V. Pakhlova, P. N. Pakhlov

Lebedev Physics Institute, 119991, Leninsky prospect 53, Moscow, Russia
National Research Nuclear University MEPhI, 115409, Kashirskoe highway 31, Moscow, Russia
Moscow Institute of Physics and Technology, 141700, Institutsky lane 9, Dolgoprudny, Moscow Region, Russia

Data on open-charm channels collected by the Belle Collaboration are analysed simultaneously using a unitary approach based on a coupled-channel model in a wide energy range $\sqrt{s} = 3.7 \div 4.7$ GeV. The resulting fit provides a remarkably good overall description of the line shapes in all studied channels. Parameters of 5 vector charmonium resonances are extracted from the fit.

1. INTRODUCTION

Four vector charmonia above the open-charm threshold, $\psi(3770)$, $\psi(4040)$, $\psi(4160)$, $\psi(4415)$, were discovered forty years ago in the e^+e^- annihilation as peaks in the total hadronic cross section [1–5]. Only thirty years later parameters of these states were updated from a naive combined fit [6] for the Crystal Ball [7] and the BES data [8]. In 2008 BES fitted the total hadronic cross section (in terms of the ratio R) [8] taking into account the interference and the relative phases between the exclusive decays of the ψ -resonances [9]. As BES used model predictions for the ψ 's decays into the two-body charmed final states, the obtained parameters remain model-dependent. In its study BES did not try to extract parameters of the vector charmoniumlike states $Y(4008)$, $Y(4260)$, $Y(4360)$, and $Y(4660)$ observed since 2005 in the e^+e^- annihilation by BaBar [10–12] and Belle [13–17] in the dipion transitions to light charmonia with the initial state radiation (ISR). Except for the $Y(4008)$ resonance found by Belle only in the $J/\psi\pi^+\pi^-$ final state, the $Y(4260)$, decaying into $J/\psi\pi^+\pi^-$, as well as the $Y(4360)$ and $Y(4660)$, decaying into $\psi(2S)\pi^+\pi^-$, are reliably established today. It has to be noticed that

the Y states lying above the open-charm threshold do not appear explicitly as peaks either in the total hadronic cross section or in the exclusive e^+e^- cross sections to the open-charm final states measured later (the only vector charmoniumlike state which reveals itself as a peak at threshold is the $X(4630)$ observed in the $\Lambda_c^+\Lambda_c^-$ final state [18].) It cannot be excluded however that some of the Y states could manifest themselves as coupled-channel effects predicted in [19].

A comprehensive study of the exclusive e^+e^- cross sections to various open-charm final states could help one to extract parameters of the ψ states in a model-independent way and therefore to shed light on the nature of the Y family. Such cross sections were first measured by Belle [18, 20–24] and BaBar [25–27] at the B -factories, using the ISR in a wide energy region $\sqrt{s} = 3.7 \div 5.0$ GeV, and by CLEO [28], using the energy scan over $\sqrt{s} = 3.97 \div 4.26$ GeV at the charm factory. BaBar performed fits to the measured two-body $D\bar{D}$, $D\bar{D}^*$, $D^*\bar{D}^*$, and $D_s^{(*)+}D_s^{(*)-}$ cross sections with the parameters of the ψ states fixed to the Particle Data Group (PDG) [29] values. From this study only the ratios of the branching fractions for the $\psi(4040)$, $\psi(4160)$, and $\psi(4415)$ decays to the $D\bar{D}$, $D\bar{D}^*$, and $D^*\bar{D}^*$ were extracted. CLEO compared the e^+e^- cross sections to

the same open-charm meson pairs with the predictions of an updated potential model [19] that appeared to fail to describe the data. Belle presented not only the two-body but also the three-body $D^0 D^{(*)-} \pi^+$ and the charmed baryon $\Lambda_c^+ \Lambda_c^-$ cross sections and demonstrated that the sum of the measured partial cross sections almost saturates the total hadronic cross section.

Many attempts were made to describe the measured exclusive cross sections [30–40]. Most of the authors [30–37] were interested in the line shape of the $\psi(3770)$ in the $e^+e^- \rightarrow D\bar{D}$ reaction while others tried to describe the $\psi(4415)$ [38, 39] or to extract the parameters of higher charmonia [40]. Although coupled-channel effects were taken into account by some authors [37–39], no simultaneous fits of all measured exclusive cross sections have been performed so far.

In this paper we present a coupled-channel fit to the exclusive cross sections of the e^+e^- annihilation to various open-charm final states. The most accurate and coherent measurements in the full \sqrt{s} interval below 5 GeV for numerous two-body final states in the e^+e^- annihilation was presented by the Belle Collaboration. The BaBar results are in a good agreement with the Belle measurements but they are incomplete for our purpose and are of a slightly worse accuracy. BES and CLEO provide measurements in several points of their energy scan which does not allow one to trace all features of the cross section in the full interval. We therefore stick to the Belle data only, available at the Durham database [41].

As was demonstrated by Belle, the sum of the four channels ($D\bar{D}$, $D\bar{D}^*$, $D^*\bar{D}^*$, $D\bar{D}\pi$) well saturates the inclusive hadronic cross section in the region $\sqrt{s} \lesssim 4.7$ GeV, so we confine ourselves by considering these four channels and this energy region only. Since the charged and the neutral modes in each channel are related to each other by the isospin symmetry which is a very accurate symmetry of QCD, we only distinguish between the D^+D^- and $D^0\bar{D}^0$ modes explicitly since they are presented separately by Belle. For the other final states only the data for the charged mode are available whose contributions are therefore doubled to mimic the presence of the neutral modes.

Then, for the $D\bar{D}\pi$ final state, Belle presented the cross section for the $D^0D^-\pi^+$ mode and demonstrated that this final state is dominated by the contribution from the two-body mode $D\bar{D}_2$. To convert the measured $D^0D^-\pi^+$ cross section into the $D\bar{D}_2$ one we correct the former by the ratio of the branching fractions $\mathcal{B}(D_2 \rightarrow D\pi)/(\mathcal{B}(D_2 \rightarrow D\pi) + \mathcal{B}(D_2 \rightarrow D^*\pi))$ [29].

Finally, when identifying the open-charm channels it should be taken into account that 3 different final

states are allowed for the $D^*\bar{D}^*$ channels, namely, the P wave with $S = 0$, the P wave with $S = 2$, and the F wave with $S = 2$. For convenience and in order to avoid confusion we count such modes as independent channels. We therefore stick to the set of 16 channels, thus counting the charge- and isospin-conjugated final states as independent ones,

$$\begin{aligned}
 D\bar{D}, & & 2 \text{ channels}, \\
 D\bar{D}^*, & & 4 \text{ channels}, \\
 D_2\bar{D}, & & 4 \text{ channels}, \\
 [D^*\bar{D}^*]_{S=0}^P, & & 2 \text{ channels}, \\
 [D^*\bar{D}^*]_{S=2}^P, & & 2 \text{ channels}, \\
 [D^*\bar{D}^*]_{S=2}^F, & & 2 \text{ channels}.
 \end{aligned} \tag{1}$$

In what follows these channels are labelled by latin letters i, j , and so on. Once the exact isospin limit is assumed, all parameters (but the charged and neutral meson masses!) in the isospin-cojugated channels are taken equal to each other.

Reactions $e^+e^- \rightarrow D^{(*)}\bar{D}^{(*)}$ studied in this work are expected to proceed through the 5 intermediate vector resonances,

$$\psi(2S), \psi(3770), \psi(4040), \psi(4160), \psi(4415), \tag{2}$$

which we denote as ψ 's and label by greek letters α, β , and so on.

The aim of the present study is to establish a proper general formalism and to determine the parameters of the vector resonances ψ enumerated in (2) from a simulations fit for all exclusive open-charm channels measured by Belle — see (1). The cornerstone of the approach used is unitarity preserved at every stage of the data analysis. This allows one to arrive at a selfconsistent description of the entire bulk of the data for the measured open-charm channels, to extract parameters of the vector ψ states in the least model-dependent way, and, in general, to establish a reliable framework for studies of various resonances simultaneously measured in several channels.

As the contributions from the charmed-strange final states or the three-body $D^*\bar{D}\pi$ final states are small and the only available data from Belle have poor accuracy for these modes, these final states are not included in the present analysis. In fact, these minor channels can also be added into the overall fit, however this would result in a significant increase of the number of free parameters which will be only very weakly constrained given a very low quality of the data in these additional channels. It is important to notice however that, while neglecting these minor channels one violates unitarity thus biasing

the result, this bias is under control due to the explicit unitarity of the approach used in this work.

2. COUPLED-CHANNEL MODEL

The traditional way to analyse the experimental data is to use individual Breit-Wigner distributions for each peak combined with a suitable background. It has to be noticed however that such an approach can provide only very limited information on the states under study. Indeed, on one hand, by analysing each reaction channel individually, one does not exploit the full information content provided by the measurements. Besides that the Breit-Wigner parameters are reaction-dependent and the naive algebraic sum of the Breit-Wigner distributions violates unitarity. The last but not the least problem with the Breit-Wigner formula is that it cannot, as a matter of principle, describe threshold phenomena which become extremely important for the studies above the open-flavour threshold.

We start from the amplitude A in the Argand units,

$$S = 1 + 2iA, \quad (3)$$

and use the K -matrix representation for it,

$$A = K(1 - iK)^{-1}, \quad (4)$$

where the K matrix is Hermitian that guarantees that the amplitude is unitary,

$$AA^\dagger = \frac{1}{2i}(A - A^\dagger). \quad (5)$$

We assume the K matrix to take the form

$$K_{ij} = \sum_{\alpha} G_{i\alpha}(s) \frac{1}{M_{\alpha}^2 - s} G_{j\alpha}(s), \quad (6)$$

where i and j run over hadronic channels and α labels the bare $\bar{c}c$ states with the masses M_{α} . The form factors $G_{i\alpha}(s)$ are defined as

$$G_{i\alpha}^2(s) = g_{i\alpha}^2 \frac{k_i^{2l_i+1}}{\sqrt{s}} \theta(s - s_i), \quad (7)$$

where $\theta(x)$ is the Heaviside step function, l_i is the angular momentum in the i -th hadronic channel and $s_i = (M_{1i} + M_{2i})^2$ is i -th threshold.

Then the amplitude A reads

$$A_{ij} = \sum_{\alpha\beta} G_{i\alpha}(s) P_{\alpha\beta}(s) G_{j\beta}(s), \quad (8)$$

with

$$(P^{-1}(s))_{\alpha\beta} = (M_{\alpha}^2 - s)\delta_{\alpha\beta} - i \sum_m G_{m\alpha} G_{m\beta}. \quad (9)$$

The couplings $g_{i\alpha}$ are defined as follows. The width $\Gamma_{i\alpha}$ for the vector ψ_{α} decaying into the i -th open-charm channel $[D^{(*)}\bar{D}^{(*)}]_i$ is given by

$$\Gamma_{i\alpha} \equiv \Gamma(\psi_{\alpha} \rightarrow [D^{(*)}\bar{D}^{(*)}]_i) = \frac{g_{i\alpha}^2}{M_{\alpha}^2} [p_i(M_{\alpha})]^{2l_i+1}, \quad (10)$$

where $p_i(M_{\alpha}) = \lambda^{1/2}(M_{\alpha}^2, m_{D_i^{(*)}}^2, m_{\bar{D}_i^{(*)}}^2)/(2M_{\alpha})$ is the centre-of-mass momentum and l_i is the angular momentum in the final state. In particular, $l_i = 1$ for $i = D^+D^-$, $D^0\bar{D}^0$, D^+D^{*-} , $[D^{*+}D^{*-}]_{S=0}^P$, and $[D^{*+}D^{*-}]_{S=2}^P$, then $l_i = 2$ for the $D_2^+D^-$ final state, and, finally, $l_i = 3$ in the $[D^{*+}D^{*-}]_{S=2}^F$ channel.

In the Vector Dominance Model (VDM), the amplitude of the annihilation process $\psi_{\alpha} \rightarrow \gamma^* \rightarrow e^+e^-$ is

$$\mathcal{M}(\psi_{\alpha} \rightarrow e^+e^-) = \frac{g_{e\alpha}}{M_{\alpha}^2} (\bar{u}\gamma_{\mu}v)\epsilon^{\mu}, \quad (11)$$

where u and v are the wave functions of the electron and positron, respectively, ϵ_{μ} is the polarisation vector of the ψ_{α} meson, M_{α} is its mass, e is the electron charge (we work in the Heaviside units, $\alpha = e^2/(4\pi)$), and $g_{e\alpha}$ is the ψ - γ coupling constant. Then the corresponding ψ_{α} 's electronic width reads

$$\Gamma_{e\alpha} \equiv \Gamma(\psi_{\alpha} \rightarrow e^+e^-) = \frac{\alpha g_{e\alpha}^2}{3M_{\alpha}^3}. \quad (12)$$

It is straightforward now to proceed to the total cross section for the annihilation process $e^+e^- \rightarrow [D^{(*)}\bar{D}^{(*)}]_i$,

$$\sigma_i(s) = \frac{4\pi\alpha}{s^{5/2}} [p_i(s)]^{2l_i+1} \left| \sum_{\alpha,\beta} g_{e\alpha} P_{\alpha\beta}(s) g_{i\beta} \right|^2, \quad (13)$$

where the inverse propagators matrix P^{-1} is defined in (9).

One can see therefore that the set of the 16 open-charm channels (1) can be described with 40 parameters,

$$\{M_{\alpha}, \Gamma_{e\alpha}, g_{i\alpha}\}, \quad \alpha = \overline{1,5}, \quad i = \overline{1,16}, \quad (14)$$

where, for convenience, we use the electronic widths $\Gamma_{e\alpha}$ as the free parameters instead of the couplings $g_{e\alpha}$ —see their interrelation in (12). As was explained above, due to the isospin symmetry, model parameters for the isospin-conjugated channels coincide with each other (except for the meson masses).

In the fitting procedure we encounter a serious problem which reveals itself in the presence the $D^*\bar{D}^*$ channel. Indeed, the transition amplitude acquires 3 independent contributions coming from the 3 different patterns for the D^* 's helicities. As was explained above, 2 of them correspond to the P wave with the total spin

equal to 0 or 2 and the third one corresponds to the F wave with $S = 2$. These 3 contributions are treated as 3 independent channels while the available experimental data provides only the sum of them all. Thus the fit is expected to have a poor capability to decompose the exclusive $D^*\bar{D}^*$ cross section into the above 3 components.

To diminish the influence of this problem we employ some heavy-quark spin symmetry (HQSS) constraints for the couplings. Namely, we use HQSS-governed P -wave spin-recoupling coefficients for both S - and D -wave vectors,

$$|^3S_1\rangle = -\frac{1}{2\sqrt{3}}|D\bar{D}\rangle + \frac{1}{\sqrt{3}}|D\bar{D}^*\rangle_- \quad (15)$$

$$|^3D_1\rangle = \frac{\sqrt{5}}{2\sqrt{3}}|D\bar{D}\rangle + \frac{\sqrt{5}}{2\sqrt{3}}|D\bar{D}^*\rangle_- + \frac{\sqrt{5}}{6}|D^*\bar{D}^*\rangle_{P0} - \frac{1}{6}|D^*\bar{D}^*\rangle_{P2}, \quad (16)$$

where $|D\bar{D}^*\rangle_-$ stands for the C -odd combination, and the subscripts $P0$ and $P2$ label the two different components of the $D^*\bar{D}^*$ P -wave function — see (1).

We assume in what follows $\psi(2S) \equiv \psi_1$, $\psi(4040) \equiv \psi_3$, and $\psi(4415) \equiv \psi_5$ to be predominantly 3S_1 states and $\psi(3770) \equiv \psi_2$ and $\psi(4160) \equiv \psi_4$ to be predominantly 3D_1 states, and relate the P -wave couplings in the $D^*\bar{D}^*$ channels,

$$g_{[D^*\bar{D}^*]_{P2,\alpha}} = -\sqrt{20}g_{[D^*\bar{D}^*]_{P0,\alpha}}, \quad \alpha = 1, 3, 5, \quad (17)$$

$$g_{[D^*\bar{D}^*]_{P0,\alpha}} = -\sqrt{5}g_{[D^*\bar{D}^*]_{P2,\alpha}}, \quad \alpha = 2, 4,$$

so that the number of the remaining free parameters of the model is reduced to 35.

It has to be noticed that the description of the same data sets in terms of the naive sums of 5 Breit-Wigners in each channel would require 15 parameters per channel (5 masses, 5 widths, 4 relative phases, and the overall norm), that is 75 parameters in total. Therefore the unitary approach used in this paper plus symmetry-driven constraints reduce the number of the free parameters by more than a factor of 2.

For the masses of the D mesons involved we use the standard PDG values [29],

$$m_{D^0} = 1864.83 \text{ MeV}, \quad m_{D^\pm} = 1869.5 \text{ MeV},$$

$$m_{D^{*0}} = 2006.85 \text{ MeV}, \quad m_{D^{*\pm}} = 2010.26 \text{ MeV}, \quad (18)$$

$$m_{D_2^\pm} = 2465.4 \text{ MeV}.$$

3. FIT FOR THE EXPERIMENTAL DATA

We have checked the consistency of the model with the experimental data and performed a simultaneous fit for the open-charm exclusive cross sections in the interval corresponding to the known ψ states. The fit minimises the function χ_{exp}^2 defined as a sum of $(\sigma_{\text{exp}} - FF)^2/\delta_{\text{exp}}^2$ over all Belle experimental points. Here FF is the Fitting Function for the given channel — see (13) — while σ_{exp} and δ_{exp} are the experimental value and the corresponding error, respectively. The statistical and systematic experimental errors of the Belle data are summed in squared.

The influence of the under-threshold $\psi(2S)$ on the $D\bar{D}$ line shape is known to be important. We therefore take into account contributions of all 5 ψ -resonances from (2) and treat the coupling constants of all 5 states to all channels as the free parameters of the fit (with the constraints from the HQSS imposed). The coupling constants to the neutral and the charged modes are set equal to each other due to the isospin symmetry and the couplings of the charge conjugated states are also considered equal to each because of the charge parity conservation. Meanwhile, due to a different phase space, the shapes of the cross sections are slightly different for the neutral and charged modes around the threshold. As the model considers only two-body final states, we assume that the $D\bar{D}\pi$ final state is dominated by the $D\bar{D}_2$ intermediate state that is consistent with the Belle study of the resonance structure in the $D\bar{D}\pi$ channels.

The $\psi(2S)$ resonance has the mass well below the threshold for the considered open-charm channels. We therefore have to fix its mass and its electronic width to the PDG values [29]. In addition, we require the $\psi(2S)$ total width to coincide with the PDG value too. To this end we add an auxiliary channel completely decoupled from the other ψ -resonances which provides the correct $\psi(2S)$ line shape near the pole mass. The coupling constants to the open-charm modes for the $\psi(2S)$ are unconstrained, so that the total number of the free parameters in the fit is eventually reduced to 33.

We constrain the fit to converge to phenomenologically adequate values, close to the PDG ones for the masses and the electronic widths of the ψ -states. Moreover, we require the total widths of the ψ -resonances to be reasonably small by adding an extra term to the χ^2 ,

$$\chi_{\text{tot}}^2 = \chi_{\text{exp}}^2 + \sum_{\alpha=1}^5 \left\{ \left(\frac{M_\alpha - M_\alpha^{\text{PDG}}}{50 \text{ MeV}} \right)^2 + \left(\frac{\Gamma_{e\alpha} - \Gamma_{e\alpha}^{\text{PDG}}}{0.5 \text{ MeV}} \right)^2 + \left(\frac{\sum_{i=1}^{16} \Gamma_{i\alpha}}{200 \text{ MeV}} \right)^2 \right\}, \quad (19)$$

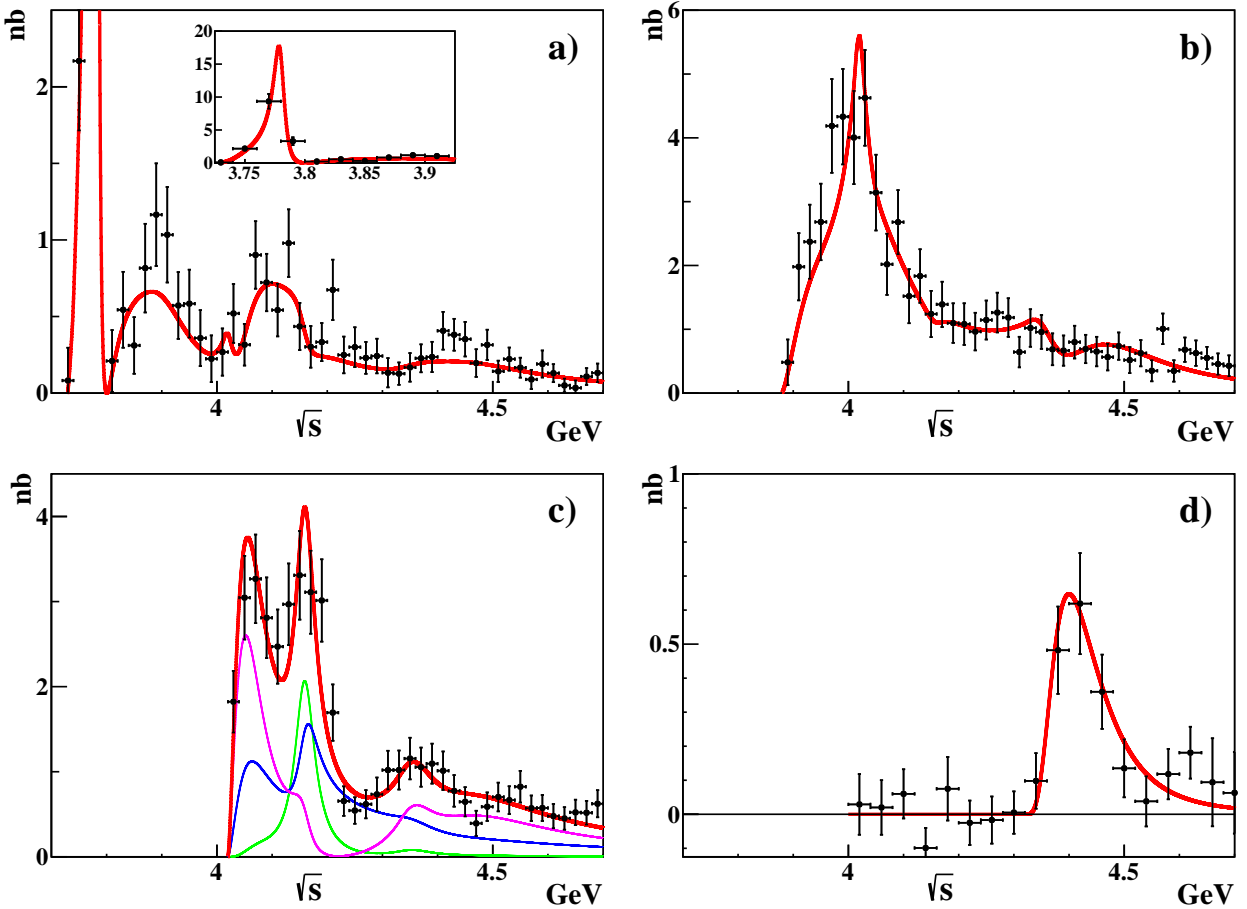


Figure 1. Exclusive cross sections for the $e^+e^- \rightarrow D\bar{D}$ ($[e^+e^- \rightarrow D^+D^-] + [e^+e^- \rightarrow D^0\bar{D}^0]$) (plot (a)), $e^+e^- \rightarrow D^+D^{*-}$ (plot (b)), $e^+e^- \rightarrow D^{*+}D^{*-}$ (plot (c)), and $e^+e^- \rightarrow D\bar{D}\pi$ ($[e^+e^- \rightarrow D^0D^-\pi^+] + [e^+e^- \rightarrow \bar{D}^0D^+\pi^-]$) (plot (d)). In all plots, the points with the error bars represent the Belle data [41] and the red curves show the fit results. In plot (c), the blue, magenta and green thin curves represent the P -wave with $S = 0$, the P -wave with $S = 2$, and the F -wave with $S = 2$ contributions in $D^{*+}D^{*-}$ final state, respectively.

where the indices i and α run over the open-charm channels and the ψ -resonances, as given in (1) and (2), respectively. The formulae for the widths are given in (10) and (12). This modification prevents the fit from blowing up the resonances and finding unphysical minima.

Finally, we fit 191 experimental points in all 5 open-charm channels with the fitting function which contains 33 free parameters. It turns out that χ_{tot}^2 possesses multiple local minima separated by barriers in the parameter space. As a result, the local minima are not continuously connected, so that the fit cannot automatically proceed from one domain, with a bad value of χ_{tot}^2 , to another domain, with a better χ_{tot}^2 . We therefore choose the following strategy to search for the global minimum. We randomly generate 10^4 seeds for the coupling constants and perform automatic fits. The initial values for the masses and the electronic widths of the ψ -resonances

are set to their respective PDG values and then they are released as free parameters. Then the fit with the best χ_{exp}^2 is selected.

The best fit found has $\chi_{\text{exp}}^2 = 158$, that is it is almost perfect, given that the number of the fitted experimental points is 191 and the number of the free parameters is 33. The line shapes which correspond to this best fit are plotted in Figs. 1 and the set of parameters is listed in Table 1. For convenience, we also quote the partial widths of the ψ 's in all studied channels — see (10).

A couple of concluding remarks on the fitting procedure are in order here. As it was mentioned above, the $\psi(2S)$ tail is an important contribution which cannot be ignored. Meanwhile, we have checked that the shape of the $\psi(2S)$ amplitude only affects the parameters of the $\psi(2S)$ coupling constants while the overall quality of the fit does not change.

The second comment is that the quality of the present data does not allow one to check how well the HQSS constraints are fulfilled in the system under study — see [42, 43] where such an analysis was performed for the near-threshold states $Z_b(10610)$ and $Z_b(10650)$ in the spectrum of bottomonium. We therefore use constraints (17) only to reduce the number of the parameters of the fit. Meanwhile, such a check should become possible for the future, more accurate, data.

4. SUMMARY

In this paper we used a coupled-channel approach to perform a simultaneous fit for the data in the major open-charm channels measured by Belle in a wide energy range $\sqrt{s} = 3.7 \div 4.7$ GeV. The main advantage of the approach used here as compared to previous works is that unitarity of the amplitude is under control at every stage of the data analysis. In particular, unitarity is preserved up to the minor contributions of the neglected strange-charm and many-body channels (we have checked that, if the model is extended to include the $D_s^+ D_s^-$ channel, then the overall description of the data improves only marginally). This allows one to link tightly the parameters in different channels and, as a result, to considerably reduce the number of free parameters of the fit. The main conclusion of the paper is that the suggested method is indeed able to explain all data sets simultaneously and provides a very good overall description of the line shapes. The presence of multiple local minima of the χ^2 should be attributed to a relatively low quality of the present data, that makes a straightforward interpretation of the parameters of the ψ -resonances extracted from the fit questionable. Meanwhile, the situation may improve considerably when the next update for the data in the open-charm channels appears.

This work is supported by the Russian Science Foundation (Grant No. 15-12-30014).

1. J. Siegrist, G. S. Abrams, A. M. Boyarski *et al.* (MARK-I Collaboration), Phys. Rev. Lett. **36**, 700 (1976).
2. P. A. Rapidis, B. Gobbi, D. Lüke *et al.* (MARK-I Collaboration), Phys. Rev. Lett. **39**, 526 (1977), Erratum-ibid. **39**, 974 (1977).
3. R. Brandelik, W. Braunschweig, H.-U. Martyn *et al.* (DASP Collaboration), Phys. Lett. B **76**, 361 (1978).
4. W. Bacino, A. Baumgarten, L. Birkwood *et al.* (DELCO Collaboration), Phys. Rev. Lett. **40**, 671 (1978).
5. R. H. Schindler, J. L. Siegrist, M. S. Alam *et al.* (MARK-II Collaboration), Phys. Rev. D **21**, 2716 (1980).
6. K. K. Seth, Phys. Rev. D **72**, 017501 (2005).
7. A. Osterheld, R. Hofstadter, R. Horisberger *et al.* (Crystal Ball Collaboration), SLAC-PUB-4160, (1986).
8. J. Z. Bai, Y. Ban, J. G. Bian *et al.* (BES Collaboration), Phys. Rev. Lett. **88**, 101802 (2002).
9. M. Ablikim, J.Z. Bai, Y. Ban *et al.* (BES Collaboration), Phys. Lett. B **660**, 315 (2008).
10. B. Aubert, R. Barate, D. Boutigny *et al.* (BaBar Collaboration), Phys. Rev. Lett. **95**, 142001 (2005).
11. B. Aubert, M. Bona, Y. Karyotakis *et al.* (BaBar Collaboration), arXiv:0808.1543, (2008).
12. B. Aubert, R. Barate, M. Bona, *et al.* (BaBar Collaboration), Phys. Rev. Lett. **98**, 212001 (2007).
13. K. Abe, K. Abe, I. Adachi *et al.* (Belle Collaboration), hep-ex/0612006.
14. C. Z. Yuan, C. P. Shen, P. Wang *et al.* (Belle Collaboration), Phys. Rev. Lett. **99**, 182004 (2007).
15. X. L. Wang, C. Z. Yuan, C. P. Shen *et al.* (Belle Collaboration), Phys. Rev. Lett. **99**, 142002 (2007).
16. X. L. Wang, C. Z. Yuan, C. P. Shen *et al.* (Belle Collaboration), Phys. Rev. D **91**, 112007 (2015).
17. Z. Q. Liu, C. P. Shen, C. Z. Yuan *et al.* (Belle Collaboration), Phys. Rev. Lett. **110**, 252002 (2013).
18. G. Pakhlova, I. Adachi, H. Aihara *et al.* (Belle Collaboration), Phys. Rev. Lett. **101**, 172001 (2008).
19. E. Eichten, K. Gottfried, T. Kinoshita, K. D. Lane, and T. M. Yan, Phys. Rev. D **21**, 203 (1980).
20. G. Pakhlova, I. Adachi, H. Aihara *et al.* (Belle Collaboration), Phys. Rev. D **77**, 011103 (2008).
21. K. Abe, I. Adachi, H. Aihara *et al.* (Belle Collaboration), Phys. Rev. Lett. **98**, 092001 (2007).
22. G. Pakhlova, I. Adachi, H. Aihara *et al.* (Belle Collaboration), Phys. Rev. Lett. **100**, 062001 (2008).
23. G. Pakhlova, I. Adachi, H. Aihara *et al.* (Belle Collaboration), Phys. Rev. D **80**, 091101 (2009).
24. G. Pakhlova, I. Adachi, H. Aihara *et al.* (Belle Collaboration), Phys. Rev. D **83**, 011101 (2011).
25. B. Aubert, R. Barate, M. Bona *et al.* (BaBar Collaboration), Phys. Rev. D **76**, 111105 (2007).
26. B. Aubert, Y. Karyotakis, J. P. Lees *et al.* (BaBar Collaboration), Phys. Rev. D **79**, 092001 (2009).
27. P. A. Sanchez, J. P. Lees, V. Poireau *et al.* (BaBar Collaboration), Phys. Rev. D **82**, 052004 (2010).
28. D. Cronin-Hennessy, K. Y. Gao, J. Hietala *et al.* (CLEO Collaboration), Phys. Rev. D **80**, 072001 (2009).
29. K.A. Olive, K. Agashe, C. Amsler *et al.* (Particle Data Group Collaboration), Chin. Phys. C **38**, 090001 (2014).
30. H. B. Li, X. S. Qin and M. Z. Yang, Phys. Rev. D **81**, 011501 (2010).
31. X. Cao and H. Lenske, arXiv:1408.5600 [nucl-th].
32. X. Cao and H. Lenske, arXiv:1410.1375 [nucl-th].
33. A. Limphirat, W. Sreethawong, K. Khosonthongkee, and Y. Yan, Phys. Rev. D **89**, 054030 (2014).

Table 1. Parameters of the ψ -resonances extracted from the fit for the Belle data. Parameters marked with the asterisk are artificially fixed to the PDG values.

	ψ_1	ψ_2	ψ_3	ψ_4	ψ_5
PDG name	$\psi(2S)$	$\psi(3770)$	$\psi(4040)$	$\psi(4160)$	$\psi(4415)$
M , MeV	3686*	3782 ± 1	4115 ± 14	4170 ± 7	4515 ± 18
Coupling constants $g_{i\alpha}$ ($\alpha = 1 \dots 5$, $i = D\bar{D}, D\bar{D}^*$, etc — see (1))					
$D\bar{D}$	3.0 ± 0.3	-1.8 ± 0.3	-0.1 ± 0.1	0.3 ± 0.1	-0.1 ± 0.1
$D\bar{D}^*$	-4.7 ± 0.5	-3.1 ± 0.3	2.4 ± 0.2	-0.0 ± 0.7	-0.7 ± 0.2
$[D^*\bar{D}^*]_{S=0}^P$	4.8 ± 0.5	6.9 ± 0.9	-0.1 ± 0.2	0.6 ± 0.5	-0.3 ± 0.1
$[D^*\bar{D}^*]_{S=2}^P$	-21.7 ± -2.3	-3.1 ± -0.4	0.5 ± 0.9	-0.3 ± -0.2	1.5 ± -0.3
$[D^*\bar{D}^*]_{S=2}^F$, MeV ⁻²	62.2 ± 15.1	-1.6 ± 5.4	-1.0 ± 2.8	8.0 ± 1.4	0.2 ± 0.6
$D_2\bar{D}$, MeV ⁻¹	-8.2 ± 29.3	25.2 ± 7.7	-23.5 ± 3.3	-1.0 ± 7.4	-1.5 ± 1.4
Partial decay widths $\Gamma_{i\alpha}$, MeV					
e^+e^-	2.354*	0.2 ± 0.0	1.6 ± 0.3	0.7 ± 0.4	1.4 ± 0.3
D^+D^-	-	5.6 ± 1.7	0.4 ± 0.8	4.3 ± 2.6	0.5 ± 1.0
$D^0\bar{D}^0$	-	7.5 ± 2.2	0.4 ± 0.8	4.5 ± 2.7	0.5 ± 1.0
D^+D^{*-}	-	-	110.7 ± 23.5	0.0 ± 0.5	32.8 ± 17.4
$[D^*\bar{D}^*]_{S=0}^P$	-	-	0.1 ± 0.2	3.6 ± 6.5	5.9 ± 2.6
$[D^*\bar{D}^*]_{S=2}^P$	-	-	1.2 ± 6.8	0.7 ± 0.3	118.0 ± 729.4
$[D^*\bar{D}^*]_{S=2}^F$	-	-	0.2 ± 1.0	58.6 ± 22.9	2.3 ± 14.2
$D_2^+D^-$	-	-	-	-	11.7 ± 21.1

34. N. N. Achasov and G. N. Shestakov, Phys. Rev. D **86**, 114013 (2012).
35. N. N. Achasov and G. N. Shestakov, Phys. Rev. D **87**, 057502 (2013).
36. Y. J. Zhang, Q. Zhao, Phys. Rev. D **81**, 034011 (2010).
37. Y. J. Zhang and Q. Zhao, Phys. Rev. D **81**, 074016 (2010).
38. J. Segovia, D. R. Entem, and F. Fernandez, Phys. Rev. D **83**, 114018 (2011).
39. J. Segovia, D. R. Entem, F. Fernandez, and E. Hernandez, Int. J. Mod. Phys. E **22**, 1330026 (2013).
40. E. van Beveren, G. Rupp, and J. Segovia, Phys. Rev. Lett. **105**, 102001 (2010).
41. Durham database, <http://durpdg.dur.ac.uk/review/rsig/BELLE.shtml>
42. C. Hanhart, Yu. S. Kalashnikova, P. Matuschek, R. V. Mizuk, A. V. Nefediev, and Q. Wang, Phys. Rev. Lett. **115**, 202001 (2015).
43. F.-K. Guo, C. Hanhart, Yu. S. Kalashnikova, P. Matuschek, R. V. Mizuk, A. V. Nefediev, Q. Wang, and J.-L. Wymen, Phys. Rev. D **93**, 074031 (2016).